Viser Technology Pte. Ltd.
Research and Application of Materials Science
https://doi.org/10.33142/msra.v1i1.671

Research Article Open Access

Solvothermal Synthesis and Visible Photocatalytic Activity of $Zn_{0.4}Cd_{0.6}S/TiO_2$/Reduced graphene oxide Nanocomposite

Yongji Shi, Botao Sun, Xinwei Wang*, Deshuang Guo

School of Materials Science and Engineering, Changchun University of Science and Technology, Changchun 130022, China

***Corresponding Author:** Xinwei Wang, wxw4122@cust.edu.cn*

Abstract:
$Zn_{0.4}Cd_{0.6}S/TiO_2$/Reduced graphene oxide ($Zn_{0.4}Cd_{0.6}S/TiO_2$/RGO) nano-photocatalyst was synthe-sized by a facile solvothermal method. During the reaction, TiO_2 and $Zn_{0.8}Cd_{0.2}S$ nanoparticles were evenly dispersed across the surface of RGO, which enhanced response to visible light. The photocatalytic activity of as-synthesized $Zn_{0.4}Cd_{0.6}S/TiO_2$/RGO nanocomposite was studied by means of degrading methylene blue (MB) through the irradiation of visible light. Compared with other nanocomposites, the $Zn_{0.4}Cd_{0.6}S/TiO_2$/RGO nanocomposite showed the highest photocatalytic degradation efficiency (96%) and high stability, which was 5.4 times of photodegradation efficiency of pure TiO_2.

Keywords: *$Zn_{0.4}Cd_{0.6}S/TiO_2$/RGO; photocatalytic activity; visible light irradiation*

Citation: Y.J. Shi, et al., Solvothermal Synthesis and Visible Photocatalytic Activity of $Zn_{0.4}Cd_{0.6}S/TiO_2$/Reduced graphene oxide Nanocomposite. *Res Appl Mat Sci*, 2019,1(1): 35-38. https://doi.org/10.33142/msra.v1i1.671

1. Introduction

Semiconductor nanomaterial photocatalysts have attracted extensive attention in recent years due to its potential applications in hydrogen production and environment pollutant degradation [1,2]. Among them, oxide semiconductors have been mainly focused in photocatalysis. However, most oxide semiconductors such as TiO_2 (E_g>3.0 eV) mainly absorb ultraviolet light due to wide band gaps, which leads to low light utilization efficiency, and even the overall process being impractical [3-5]. As we all know, ultraviolet light only occupies about 4% of the solar spectrum, while visible light possesses 43% [6-9]. Therefore, increasing the availability of visible light for the practical application of photocatalyst still is now a challenge. $Zn_xCd_{1-x}S$, as a typical alloyed chalcogenide semiconductor, is a promising material due to its remarkable properties such as excellent electrical conductivity, valence bands at relatively negative potentials [10-13]. Therefore, it can be applied in photocatalysis, particularly in the visible light driven photocatalytic degradation of dyes. Furthermore, the rapid recombination of the excited electron-hole pairs is also an obstacle limiting the photocatalytic activity of catalysts. To solve the problem, various investigations have been carried out to improve the efficiency of the photocatalytic activity for single semiconductor [14-18].

Two-dimensional graphene as a promising material is widely used in the field of photocatalysis because of large specific surface area, and high carrier mobility [9]. The researchers have actively used different experimental methods or techniques to combine various semiconductor nanocomposites with graphene or reduced graphene oxide (RGO) to effectively improve their photocatalytic properties [19-21].

Therefore, TiO_2, $Zn_{0.4}Cd_{0.6}S/TiO_2$, $Zn_{0.4}Cd_{0.6}S/TiO_2$/RGO nanocomposites are synthesized via a facile solvothermal process. And these synthesized nanocomposites as typical photocatalysts is studied for their photodegradation activity, in which methylene blue (MB) is selected as probe material to determine the photocatalytic properties of synthesized nanocomposites under visible light irradiation.

2. Experimental

Photocatalysts synthesis: Since preliminary studies showed that the $Zn_xCd_{1-x}S$ nanoparticles (x=0.4) without graphite oxide (GO), namely, $Zn_{0.4}Cd_{0.6}S$ exhibited highest photodegradation activity [19]. GO was synthesized by classical modified Hummers experimental methods by natural graphite powder as carbon source [14]. The a typical synthesis process of the $Zn_{0.4}Cd_{0.6}S/TiO_2$/RGO nanocomposites is as follows: firstly, 329 mg $Zn(Ac)_2{\cdot}2H_2O$ (as Zn source), 100 mg $Cd(Ac)_2{\cdot}2H_2O$ (as Cd source), and 150 mg $TiCl_3$ (as Ti source) were added to 100 mL DMSO solution (as S source).Then, the suspension solution was vigorously stirred, and the 100 mg GO was put in it for 3 h. Afterward, the suspen-

sion solution was transferred into a Teflon-lined autoclave (200 mL) to react 12 h at 180℃. The reaction products were cleaned in turn by ethanol and deionized water, and then dried at 60℃ under vacuum. In addition, pure TiO_2 (or $Zn_{0.4}Cd_{0.6}S/TiO_2$) was also synthesized by the above method in the absence of GO (or $Zn_{0.4}Cd_{0.6}S$).

Characterization: X-ray diffraction (XRD) patterns of the powders were carried out by means of a Bruker D8 Advance X-ray diffractometer. To exhibt the morphologies and structures of samples, transmission electron microscope (TEM) (JOEL TEM-2010) with a field emission gun operating at 200 kV were employed. UV-vis spectrophotometer (Shimadzu, UV3600) was used to test UV-vis diffuse reflectance spectra and the concentration changes of MB of the samples.

Photocatalytic experiment: To evaluate photocatalytic activities of as-prepared samples, the degradation experiment for MB solution was carried out under visible light irradiation (λ > 420 nm). First, as-prepared samples (50 mg) was completely dispersed into 0.01 mM/100 mL MB solution. Then dispersed solution was continuously stirred with the help of 300W Xe lamp with light filter (420nm). And, the suspension was stirred in dark for 1 h to reach adsorption-desorption equilibrium. The reusability experiments of the sample were also tested by reusing the photocatalyst with the same experimental conditions.

3. Results and Discussion

Figure 1a shows the XRD patterns of TiO_2, $Zn_{0.4}Cd_{0.6}S$, and $Zn_{0.4}Cd_{0.6}S/TiO_2$/RGO nanocomposites. $Zn_{0.4}Cd_{0.6}S$ and TiO_2 exhibite sphalerite phase [JCPDS No. 05-0566] and anatase phase [JCPDS No.71-1166], respectively. $Zn_{0.4}Cd_{0.6}S/TiO_2$/RGO shows mixed crystal phase in which include correlative characteristic peaks of $Zn_{0.4}Cd_{0.6}S$ and TiO_2. Otherwise, no apparent peaks of RGO are observed in $Zn_{0.4}Cd_{0.6}S/TiO_2$/RGO nanocomposite because of its lower loading content and weak crystallization.

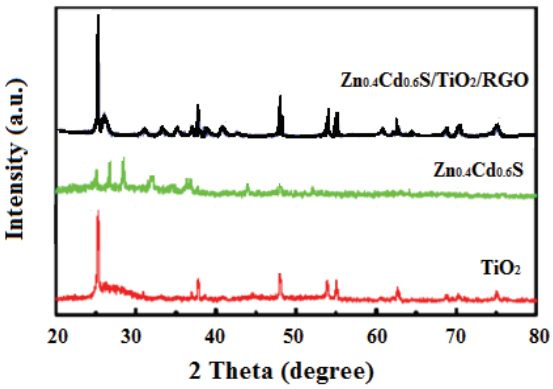

Figure 1. X-ray diffraction patterns of TiO_2, $Zn_{0.4}Cd_{0.6}S$, and $Zn_{0.4}Cd_{0.6}S/TiO_2$/RGO nanocomposites.

Figure 2 shows TEM image of $Zn_{0.4}Cd_{0.6}S/TiO_2$/RGO nanocomposite. From the image, we can see that $Zn_{0.4}Cd_{0.6}S$ and TiO_2 are nanospheres composing of smaller nanoparticles (Figure 2). Furthermore, these nanospheres are homogeneously scattered on RGO, indicating a strong interaction between these nanospheres of $Zn_{0.4}Cd_{0.6}S$, TiO_2 and RGO support to be propitious to catalytic activity.

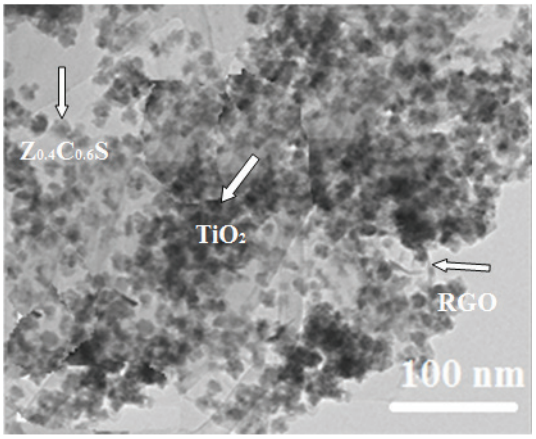

Figure 2. TEM image of $Zn_{0.4}Cd_{0.6}S/TiO_2$/RGO nanocomposite.

The UV-vis diffused reflectance spectra of TiO_2, $Zn_{0.4}Cd_{0.6}S/TiO_2$, and $Zn_{0.4}Cd_{0.6}S/TiO_2$/RGO nanocomposites are also shown in Figure 3. As can be seen, the onset wavelength for TiO_2, $Zn_{0.4}Cd_{0.6}S/TiO_2$, and $Zn_{0.4}Cd_{0.6}S/TiO_2$/RGO are ca.375 nm, 480 nm, and 550 nm respectively, corresponding to a bandgap of 3.31 eV, 2.58 eV, and 2.25 eV. We have estimated the bandgap energy of synthesized samples via extrapolating the straight portion of the $(ahv)^2$ versus photon energy (h) curve to a=0, in which a is absorption coefficient, h is Planck's constant, and v is frequency from the Kubelka-Munk function [15,16]. In addition, the absorbance intensity and region of $Zn_{0.4}Cd_{0.6}S/TiO_2$/RGO nanocomposite obviously enhance and broaden with the induction of RGO in the rang of visible light (>500 nm), which can be attributed to the full absorption of RGO for visible light. Therefore, we can infer that the prepared nanocomposites are suitable for visible-light response.

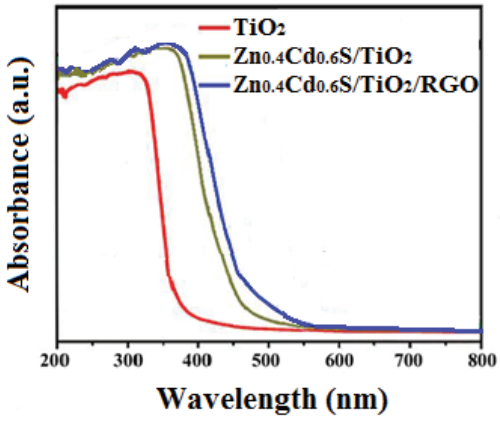

Figure 3. UV-vis diffuse reflectance spectra of TiO_2, $Zn_{0.4}Cd_{0.6}S/TiO_2$, and $Zn_{0.4}Cd_{0.6}S/TiO_2$/RGO nanocomposites.

The photocatalytic activities of $Zn_{0.4}Cd_{0.6}S$, $Zn_{0.4}Cd_{0.6}S/TiO_2$, and $Zn_{0.4}Cd_{0.6}S/TiO_2$/RGO nanocomposite are measured by the photodegradation of MB in aqueous solution under visible light irradiation (λ > 420 nm). The results are shown in Figure 4a and b, respectively. It is clear that the photocatalytic activity of pure $Zn_{0.4}Cd_{0.6}S$ is low, only 18% of MB is degraded. The photodegradation activities of $Zn_{0.4}Cd_{0.6}S/TiO_2$, and $Zn_{0.4}Cd_{0.6}S/TiO_2$/RGO nanocomposite are significantly enhanced compared with $Zn_{0.4}Cd_{0.6}S$. This indicate that higher photocatalytic activity is achieved due to intimate contact between $Zn_{0.4}Cd_{0.6}S$, TiO_2, and RGO, which is beneficial to interelectron transfer at the in-

terface. Notably, the photocatalytic activity of $Zn_{0.4}Cd_{0.6}S/TiO_2$/RGO nanocomposite increases quickly with induction of RGO, and which reaches the optimum activity, namely, the highest photodegradation efficiency 98 % after 120 min, which is 5.4 times that of pure $Zn_{0.4}Cd_{0.6}S$. Their photodegradation efficiency show as follows (Figure4a): $Zn_{0.4}Cd_{0.6}S/TiO_2$/RGO > $Zn_{0.4}Cd_{0.6}S/TiO_2$> $Zn_{0.4}Cd_{0.6}S$. In addition, to effectively demonstrate the degradation efficiency, the photodegradation kinetic process of $Zn_{0.4}Cd_{0.6}S/TiO_2$/RGO was also investigated for MB. The kinetic reacting process are fitted to a pseudo first-order reaction at low dye concentrations. This reaction follows the following formula:

$$\ln(C_0/C) = kt$$

C_0 is the initial concentration and C is the measured concentration, while k correspond to the photodegradation rate constant for the MB solution at reaction time t. As can be seen in Figure4b, the order of the k values is summarized as follows: $Zn_{0.4}Cd_{0.6}S/TiO_2$/RGO (k=0.0309)> $Zn_{0.4}Cd_{0.6}S/TiO_2$ (k=0.0295)> $Zn_{0.4}Cd_{0.6}S$ (k=0.0178). It is well coincident with the results presented in Figure4b. The photocatalytic enhancement of the $Zn_{0.4}Cd_{0.6}S/TiO_2$/RGO nanocomposite may be attributed to the introduction of both TiO_2 and RGO can simultaneously promote the migration of photogenerated electrons and holes from $Zn_{0.4}Cd_{0.6}S$ to space separated active sites on RGO and TiO_2, respectively, thus greatly suppressing their recombination and increasing their lifetime. Among them, TiO_2 nanoparticles can not only assemble the photogenerated holes from $Zn_{0.4}Cd_{0.6}S$ but also act as oxidation active sites to facillitate the irreversible consumption of the holes by sacrificial reagents, while the photogenerated electrons can be further enriched in the conduction band of $Zn_{0.4}Cd_{0.6}S$. In addition, the unique features of RGO nanosheets can effectively collect the photogenerated electrons from the conduction band of $Zn_{0.4}Cd_{0.6}S$, prolong the lifetime of the photogenerated electrons and enlarge the reduction reaction space, thus enhacing the photocatalytic activity of the $Zn_{0.4}Cd_{0.6}S/TiO_2$/RGO nanocomposite[22].

Furthermore, to evaluate the photostability, We have performed three cyclic photocatalytic degradation experiments for the $Zn_{0.4}Cd_{0.6}S/TiO_2$/RGO nanocomposite under the same experimental conditions (Figure 5). After 3 consecutive cycles, the photocatalytic degradation efficiency of $Zn_{0.4}Cd_{0.6}S/TiO_2$/RGO nanocomposite did not decrease significantly for the photodegradation of MB, which fully indicates that the structure of the $Zn_{0.4}Cd_{0.6}S/TiO_2$/RGO is optical stability and does not suffer from photocorrosion in the process of photodegradation.

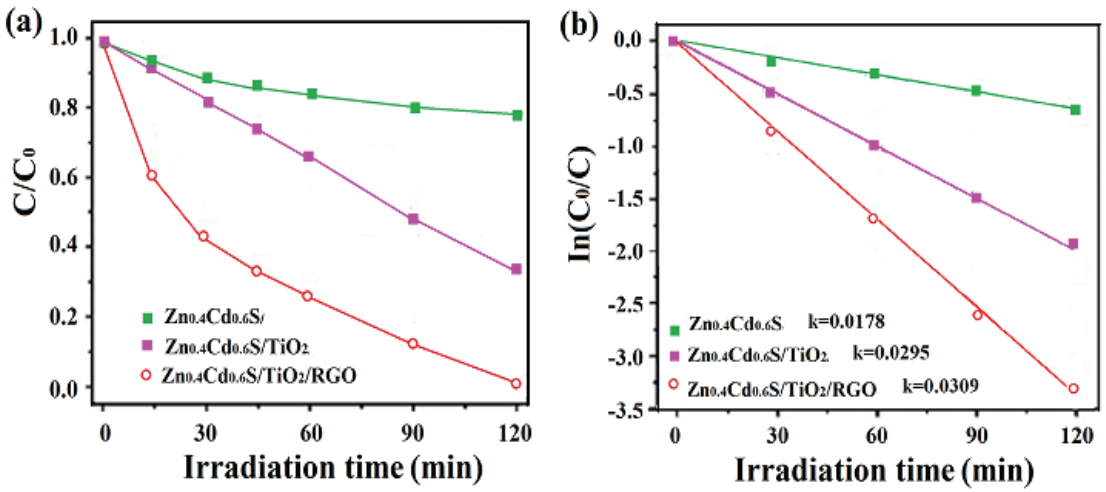

Figure 4. Photodegradation of MB (a) and the kinetics of photodegradation of MB (b) by different photocatalysts under visible light.

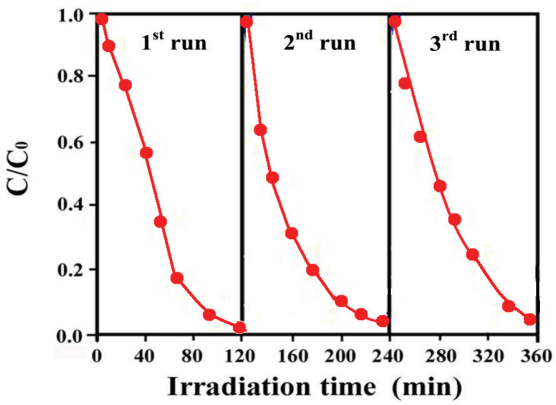

Figure 5. Recycling runs in the photodegradation of MB with $Zn_{0.4}Cd_{0.6}S/TiO_2$/RGO under the visible-light irradiation

4. Conclusions

we have developed a solvothermal method for the synthesis of $Zn_{0.4}Cd_{0.6}S/TiO_2$/RGO nano-photocatalysts, which showed that $Zn_{0.4}Cd_{0.6}S$ and TiO_2 nanoparticles can be distributed homogeneously on RGO surface. Besides, $Zn_{0.4}Cd_{0.6}S/TiO_2$ nanocomposite had much higher photocatalytic activity than pure TiO_2 nanoparticles for MB degradation. Among them, the $Zn_{0.4}Cd_{0.6}S/TiO_2$/RGO exhibited the highest photocatalytic activity, which is 5.4 times of pure TiO_2 nanoparticles.

Acknowledgments: This work is supported by the Innovation Foundation of Changchun University of Science and Technology (XJJLG-2016-11, XJJLG-2016-14) and the Foundation of NANOX (18JG01)..

References

[1] Woan K, Pyrgiotakis G, Sigmund W. Photocatalytic carbon-nanotube-TiO_2 composites[J]. Advanced Materials, 2009, 21(21): 2233-2239.

[2] Yu J, Zhang J, Jaroniec M. Preparation and enhanced visible-light photocatalytic H_2-production activity of CdS quantum dots-sensitized $Zn_{1-x}Cd_xS$ solid solution[J]. Green Chemistry, 2010, 12(9): 1611-1614.

[3] Cui L, Hui KN, Hui KS, et al. Facile microwave-assisted hydrothermal synthesis of TiO_2 nanotubes[J]. Materials Letters, 2012, 75: 175-178.

[4] Etacheri V, Di Valentin C, Schneider J, et al. Visible-light activation of TiO_2 photocatalysts: Advances in theory and experiments[J]. Journal of Photochemistry and Photobiology C: Photochemistry Reviews, 2015, 25: 1-29.

[5] Truong QD, Liu JY, Chung CC, et al. Design and fabrication of semiconductor photocatalyst for photocatalytic reduction of CO_2 to solar fuel[J]. Catal. Commun, 2012, 19: 8589.

[6] Li YX, Chen G, Wang Q, et al. Hierarchical ZnS-In_2S_3-CuS Nanospheres with Nanoporous Structure: Facile Synthesis, Growth Mechanism, and Excellent Photocatalytic Activity[J]. Advanced Functional Materials, 2010, 20(19): 3390-3398..

[7] Wang W, Germanenko I, El-Shall M S. Room-temperature synthesis and characterization of nanocrystalline CdS, ZnS, and $Cd_xZn_{1-x}S$[J]. Chemistry of Materials, 2002, 14(7): 3028-3033.

[8] Xing CJ, Zhang YJ, Yan W, et al. Band structure-controlled solid solution of $Cd_{1-x}Zn_xS$ photocatalyst for hydrogen production by water splitting[J]. International Journal of Hydrogen Energy, 2006, 31(14): 2018-2024.

[9] Xu X, Lu RJ, Zhao XF, et al. Novel mesoporous $Zn_xCd_{1-x}S$ nanoparticles as highly efficient photocatalysts[J]. Applied Catalysis B: Environmental, 2012, 125: 11-20.

[10] Wu HQ, Yao YZ, Li WT, et al. Microwave-assisted synthesis of $Zn_xCd_{1-x}S$ -MWCNT heterostructures and their photocatalytic properties[J]. Journal of Nanoparticle Research, 2011, 13(5): 2225-2234.

[11] Li WJ, Li DZ, Meng SG, et al. Novel Approach To Enhance Photosensitized Degradation of Rhodamine B under Visible Light Irradiation by the $Zn_xCd_{1-x}S$ /TiO_2 Nanocomposites[J]. Environmental science & technology, 2011, 45(7): 2987-2993.

[12] Novoselov KS, Geim AK. The rise of graphene[J]. Nat. Mater, 2007, 6(3): 183-191.

[13] Xiang Q, Yu J, Jaroniec M. Graphene-based semiconductor photocatalysts[J]. Chemical Society Reviews, 2012, 41(2): 782-796.

[14] Ping JF, Fan ZX, Sindoro M, et al. Recent advances in sensing applications of two - dimensional transition metal dichalcogenide nanosheets and their composites[J]. Advanced Functional Materials, 2017, 27(19): 1605817.

[15] Lu QP, Yu YF, Ma QL, et al. 2D Transition- metal- dichalcogenide- nanosheet- based composites for photocatalytic and electrocatalytic hydrogen evolution reactions[J]. Advanced Materials, 2016, 28(10): 1917-1933.

[16] An X, Jimmy C Y. Graphene-based photocatalytic composites[J]. Rsc Advances, 2011, 1(8): 1426-1434.

[17] Lou SY, Wang YQ, Zhou SM, et al. A facile method to immobilize $Zn_xCd_{1-x}S$ nanocrystals on graphene nanoribbons[J]. Materials Letters, 2012, 67(1): 169-172.

[18] Zhang J, Yu JG, Jaroniec M, et al. Noble metal-free reduced graphene oxide -$Zn_xCd_{1-x}S$ nanocomposite with enhanced solar photocatalytic H_2-production performance[J]. Nano letters, 2012, 12(9): 4584-4589.

[19] Wang XW., Tian HW., Cui XQ., Zheng W.T., Liu Y.C., "One-pot hydrothermal synthesis of mesoporous $Zn_xCd_{1-x}S$/reduced graphene oxide hybrid material and its enhanced photocatalytic activity", Dalton Trans., 2014,43:12894-12903.

[20] Zhou MH, Yu JG. Preparation and enhanced daylight -induced photocatalytic activity of C, N, S- tridoped titanium dioxide powders[J]. Journal of Hazardous Materials, 2008, 152: 1229–1236

[21] Kubelka, P. J. New contributions to the optics of intensely light-scattering materials. Part I Paul Kubelka [J]. Journal of the Optical Society of America, 1948, 38(5): 448-457.

[22] Zhang J, Qi LF, Ran JR, Yu JG, Qiao SZ. Ternary NiS/$Zn_xCd_{1-x}S$/reduced graphene oxide nanocomposites for enhanced solar photocatalytic H_2-production activity [J]. Advanced Energy Materials., 2014, 4: 1301925-1301930.